Inferring directional interactions from transient signals with symbolic transfer entropy

Marcel Martini,[1,2,*] Thorsten A. Kranz,[1,2] Tobias Wagner,[1,2] and Klaus Lehnertz[1,2,3,†]

[1]*Department of Epileptology, University of Bonn, Sigmund-Freud-Strasse 25, D-53105 Bonn, Germany*

[2]*Helmholtz-Institute for Radiation and Nuclear Physics, University of Bonn, Nussallee 14-16, D-53115 Bonn, Germany*

[3]*Interdisciplinary Center for Complex Systems, University of Bonn, Brühlerstrasse 7, D-53119 Bonn, Germany*

(Received 6 October 2010; published 28 January 2011)

We extend the concept of symbolic transfer entropy to enable the time-resolved investigation of directional relationships between coupled dynamical systems from short and transient noisy time series. For our approach, we consider an observed ensemble of a sufficiently large number of time series as multiple realizations of a process. We derive an index that quantifies the preferred direction of transient interactions and assess its significance using a surrogate-based testing scheme. Analyzing time series from noisy chaotic systems, we demonstrate numerically the applicability and limitations of our approach. Our findings obtained from an analysis of event-related brain activities underline the importance of our method to improve understanding of gross neural interactions underlying cognitive processes.

DOI: 10.1103/PhysRevE.83.011919 PACS number(s): 87.19.lm, 02.50.−r, 05.45.Tp

I. INTRODUCTION

Inferring interactions between complex dynamical systems is of importance in many scientific disciplines, ranging from physics, chemistry, biology, meteorology, and economy to the neurosciences. Because the underlying equations of motion are usually not known, a number of time-series analysis techniques have been developed that aim at a quantitative description of interactions from experimentally acquired observables. While most of these techniques allow one to quantify the strength of interactions [1–3], the more recent developments of asymmetric approaches have facilitated the characterization of the direction of interactions from time series. These approaches include parametric and nonparametric spectral methods [4–6], techniques based on interrelations of phases [7–17], state-space-based methods [18–25], methods based on the concept of Granger causality [26–28] or on the Fokker-Planck formalism [29,30], as well as information-theoretic techniques [31–34]. Within the latter framework, transfer entropy [35] has been proposed to distinguish effectively the driving and responding elements and to detect asymmetry in the interaction of subsystems. Various techniques have been proposed to estimate transfer entropy from observed data [36–40], among which symbolic transfer entropy [41] has been shown to allow a convenient, robust, and computationally fast quantification of the dominating direction of information flow between time series.

Almost all of the aforementioned linear and nonlinear analysis techniques require rather long time series to reliably estimate the strength or the direction of interactions. Acquiring long time series from natural systems, however, is often impossible owing to experimental restrictions. Moreover, in many systems relevant interactions may occur on quite short time scales (e.g., with extreme events such as earthquakes or epileptic seizures), rendering the recording of long time series unfeasible. In such situations, moving window techniques are commonly used to track time-dependent interactions but their temporal resolution is still limited depending on the window's length. More recently, techniques had been developed that allow a time-resolved estimation of strength and direction of an interaction in cases where multiple realizations of the corresponding transient dynamics are available [42–47]. Similar techniques have been used already for the detection of transient chaos [48,49] and for the nonlinear denoising of transient signals [50,51]. Here we follow this line of approach and propose a method for the time-resolved estimation of symbolic transfer entropy, particularly with respect to field applications.

This paper is organized as follows. In Sec. II A we briefly recall the definition of symbolic transfer entropy, and in Sec. II B we present our approach to detect directional couplings with high temporal resolution, given a sufficient number of realizations of the processes under investigation. Next, we present our numerical simulation studies that aim at an exploration of the limitations of our method (Sec. III A). In Sec. III B we investigate directed interactions in event-related neuroelectric activities before we draw our conclusions in Sec. IV.

II. METHODS

A. Symbolic transfer entropy

Let $i_n = i(n)$ and $j_n = j(n)$, $n = 1, \ldots, N$ denote sequences of observations from systems I and J. Transfer entropy [35] is related to the concept of Granger causality in the sense that it incorporates time dependency by relating previous samples i_n and j_n to predict the next value i_{n+1}, and it has been shown that Granger causality and transfer entropy are equivalent for Gaussian variables [52]. Transfer entropy specifies the deviation from the generalized Markov property, $p(i_{n+1}|i_n, j_n) = p(i_{n+1}|i_n)$, where p denotes the transition probability density. If there is no deviation, J has no influence on I. Transfer entropy quantifies the incorrectness of this assumption, and is explicitly nonsymmetric under the exchange of i_n and j_n.

In order to estimate the transition probabilities p, Staniek and Lehnertz [41] proposed to convert the sequences of

*marcel.martini@gmx.de

†klaus.lehnertz@ukb.uni-bonn.de

observations i_n and j_n into a sequence of symbols $S(I_n)$ and $S(J_n)$ by using a permutation technique [53]. For a given but otherwise arbitrary n, w amplitude values $I_n = \{i_n, i_{n+\tau}, \ldots, i_{n+(w-1)\tau}\}$ can be reordered in an increasing order $\{i_{n+(k_1-1)\tau} \leqslant i_{n+(k_2-1)\tau} \leqslant \ldots \leqslant i_{n+(k_w-1)\tau}\}$, where τ denotes the time delay, and w is the embedding dimension. Thus, every I_n is uniquely mapped onto one of the $w!$ possible permutations, and a symbol can be defined as $S(I_n) \equiv (k_1, k_2, \ldots, k_w)$. Joint and conditional probabilities can then be estimated using the relative frequency of these symbols. Given a symbol sequence $S(I_n)$ and an analogous defined symbol sequence $S(J_n)$, symbolic transfer entropy (STE) then reads [41]

$$\tilde{T}_{J\to I} = \sum p(S(i_{n+1}), S(i_n), S(j_n)) \times \log_2 \frac{p(S(i_{n+1})|S(i_n), S(j_n))}{p(S(i_{n+1})|S(i_n))}. \quad (1)$$

The sum runs over the sequence of symbols, and $\tilde{T}_{I\to J}$ is defined in complete analogy.

B. Time-resolved detection of directional couplings with STE

A reliable estimation of STE requires a sufficient amount of data points N ($N > w!$), which hinders the time-resolved detection of directional couplings. In Refs. [43,46,47] techniques had been proposed that allow one to detect transient directional interactions in cases where an ensemble of a sufficiently large number of time series as multiple realizations of a process is available. Here we follow this line of approach and propose to estimate STE, at each time point n, from the distribution of permutation symbols within an ensemble of R realizations $I_n^{(r)}$ and $J_n^{(r)}$, $r = 1, \ldots, R$. In analogy to Eq. (1), our time-dependent STE then reads

$$\tilde{T}_{J\to I}(n) = \sum p\left(S\left(i_{n+1}^{(r)}\right), S\left(i_n^{(r)}\right), S\left(j_n^{(r)}\right)\right) \times \log_2 \frac{p\left(S\left(i_{n+1}^{(r)}\right)\middle|S\left(i_n^{(r)}\right), S\left(j_n^{(r)}\right)\right)}{p\left(S\left(i_{n+1}^{(r)}\right)\middle|S\left(i_n^{(r)}\right)\right)}, \quad (2)$$

where the sum runs over the ensemble of realizations (for each n). With this definition the reliability of $\tilde{T}_{J\to I}(n)$ does not depend on the number of data points N but on the number of realizations R of the processes. Directional interactions can thus be inferred on very short time scales and with only a few data points if a sufficient number of realizations is available. Here we are interested in the preferred direction of information flow and thus define the time-resolved directionality index (cf. Ref. [41])

$$\Delta T(n) = \tilde{T}_{I\to J}(n) - \tilde{T}_{J\to I}(n). \quad (3)$$

Here, $\Delta T(n) > 0$ for unidirectional couplings with I as the driver and $\Delta T(n) < 0$ for J driving I. When analyzing the field data, however, it is quite difficult to judge whether a nonzero value of $\Delta T(n)$ unequivocally reflects unidirectional couplings. In order to minimize false interpretations, we follow Refs. [43,47] and use a surrogate-based testing scheme. Under the null hypothesis that the dynamics of systems I and J are independent, the surrogates are designed such that they preserve the temporal structure of each time series and destroy the dependence between systems. To test if the process of system I is independent on that of system J, we randomly permute the realizations of system J and keep those of system I fixed. We generate M surrogates and denote their time-dependent STE values with $\tilde{T}^s_{J\to I}(n)$. Values for $\tilde{T}^s_{I\to J}(n)$ are derived in complete analogy. With $\Delta T^s_{\min}(n) = \min(\tilde{T}^s_{I\to J}(n)) - \max(\tilde{T}^s_{J\to I}(n))$ and $\Delta T^s_{\max}(n) = \max(\tilde{T}^s_{I\to J}(n)) - \min(\tilde{T}^s_{J\to I}(n))$, we consider $\Delta T(n)$ to reflect the preferred direction of information flow if $\Delta T(n) \notin [\Delta T^s_{\min}(n), \Delta T^s_{\max}(n)]$.

III. APPLICATIONS

A. Coupled Lorenz systems

We studied two diffusively coupled Lorenz systems X and Y [54]:

$$\begin{aligned}
\dot{x}_1^{(r)}(n) &= 10\left[x_2^{(r)}(n) - x_1^{(r)}(n)\right] + C_2\left[y_1^{(r)}(n) - x_1^{(r)}(n)\right],\\
\dot{x}_2^{(r)}(n) &= x_1^{(r)}(n)\left[(R_L + \epsilon) - x_3^{(r)}(n)\right] - x_2^{(r)}(n),\\
\dot{x}_3^{(r)}(n) &= x_1^{(r)}(n)x_2^{(r)}(n) - \tfrac{8}{3}x_3^{(r)}(n),\\
\dot{y}_1^{(r)}(n) &= 10\left[y_2^{(r)}(n) - y_1^{(r)}(n)\right] + C_1\left[x_1^{(r)}(n) - y_1^{(r)}(n)\right],\\
\dot{y}_2^{(r)}(n) &= y_1^{(r)}(n)\left[(R_L + \epsilon) - y_3^{(r)}(n)\right] - y_2^{(r)}(n),\\
\dot{y}_3^{(r)}(n) &= y_1^{(r)}(n)y_2^{(r)}(n) - \tfrac{8}{3}y_3^{(r)}(n).
\end{aligned} \quad (4)$$

We generated an ensemble of R realizations of the systems by randomly choosing the initial conditions in state space near the Lorenz attractor and by randomly adding tiny variations $\epsilon \in [-0.04, 0.04]$ to the control parameter $R_L = 28$. The equations of motion were integrated using a fourth-order Runge-Kutta algorithm [55] with a step size of 0.001 and a sampling interval of 0.01. For our analyses we generated time series of the first components with $N = 2500$ data points each after 5×10^4 transients. With the coupling strengths C_1 and C_2 we realized time-variant diffusive couplings between oscillators such that $C_1 = 5 \wedge C_2 = 0$ for $n \in [500, 999]$, $C_1 = 0 \wedge C_2 = 5$ for $n \in [1500, 1999]$, and $C_1 = C_2 = 0$ for $n \in [0, 499]$ or $n \in [1000, 1499]$ or $n \in [2000, 2499]$. We chose $w = 4$ and $\tau = 6$ [56] to estimate the time-resolved directionality index $\Delta T(n)$.

The temporal evolution of $\Delta T(n)$ obtained from $R = 500$ realizations of the systems reflects, despite large fluctuations, the coupling changes (cf. Fig. 1). For time intervals with a nonzero coupling strength, we observe—as expected—$\Delta T(t)$ to increase (for the case $C_1 = 5 \wedge C_2 = 0$) or to decrease (for the case $C_1 = 0 \wedge C_2 = 5$) rapidly after the onset of the coupling and then to deviate from the surrogates until the coupling is switched off. Hence the null hypotheses of the Lorenz systems being independent is correctly rejected for most samples. For time intervals with zero coupling strengths, $\Delta T(n)$ fluctuates at approximately zero but remains well within the range of the surrogates. The null hypothesis thus cannot be rejected and the systems are correctly detected as noninteracting.

Given the large fluctuations seen in the temporal evolution of $\Delta T(n)$, we estimated the relative number of true and false detections of the coupling direction. For the cases $C_1 = 5 \wedge C_2 = 0$ and $C_1 = 0 \wedge C_2 = 5$, we denote with f_{td} the relative number of samples for which the coupling direction could be correctly detected using our surrogate-based testing scheme. With f_{fd} we denote the relative number of samples in

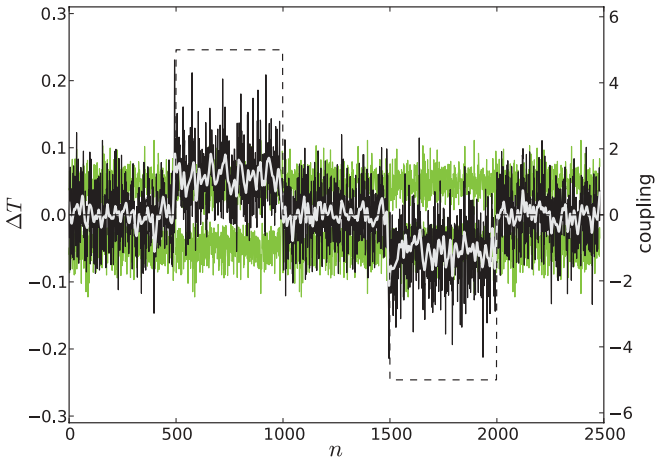

FIG. 1. (Color online) Exemplary temporal evolution of directionality index $\Delta T(n)$ (black line, a moving average over 20 data points is shown as a light gray line) and of extreme values [$\Delta T^s_{\min}(n)$ and $\Delta T^s_{\max}(n)$; green lines] derived from $M = 19$ surrogates for an ensemble of $R = 500$ realizations of coupled Lorenz systems. The time-variant coupling strengths are shown as black dotted lines.

the temporal evolution of $\Delta T(n)$ for which our testing scheme mistakenly detected a coupling direction (i.e., for the case $C_1 = C_2 = 0$) or for which a nonzero coupling could not be detected (note that f_{td} and f_{fd} do not necessarily add up to 1 because we consider different parent populations for true and false detections). For the example shown in Fig. 1, we obtained $f_{\text{td}} = 71\%$ and $f_{\text{fd}} = 15\%$. We note that the number of true and false detections can be improved by using a higher number of surrogates.

In order to estimate the performance of our approach, particularly with respect to the analysis of empirical data, we investigated the impact of observational noise and the number of realizations R on the inference of directional relationships. We repeated the analyses for coupled Lorenz systems as outlined above for different numbers of realizations $R \in [100, 2000]$ and varied the amount of noise contamination (additive Gaussian δ-correlated noise; the noise-to-signal ratio is $\rho = \sigma^2_{\text{noise}}/\sigma^2_{\text{signal}}$). In Fig. 2 we show the relative number of true (f_{td}) and false detections (f_{fd}) of the coupling direction depending on the ensemble size R and on the noise-to-signal ratio ρ. We first consider the case of noise contaminations to be equal for both systems ($\rho_X = \rho_Y$). For the noise-free case, f_{td} increases while f_{fd} decreases monotonically with an increasing ensemble size R. For the coupled Lorenz systems investigated here we achieve an unequivocal detection of the coupling direction ($f_{\text{td}} \to 1$, $f_{\text{fd}} \to 0$) for $R \geqslant 2000$. For small ensemble sizes ($R \leqslant 200$) the relative number of true detections drops below 0.5 and the coupling direction cannot be resolved anymore. As expected, f_{td} decreases while f_{fd} increases monotonically with an increasing noise-to-signal ratio. Nevertheless, even for the case $\rho = 100\%$, a large enough ensemble size ($R \geqslant 2000$) allows the coupling direction to be resolved with a detection rate above chance level.

Next, we consider the case of asymmetric noise contaminations ($\rho_X \neq \rho_Y$) that is more likely in field applications and is known to affect various time-series analysis techniques, aiming at an inference of directional interactions [8,20,24,57,58]. In Fig. 3 we present our findings for the coupled Lorenz systems with a fixed ensemble size $R = 2000$. We observe f_{td} to decrease and f_{fd} to increase monotonically with increasing noise-to-signal ratios. Obviously, detection rates depend on the sum of the amount of noise in both systems only, no matter how it is distributed. This indicates that our analysis technique does not identify the signal with the highest (lowest) noise-to-signal ratio as the most influential one.

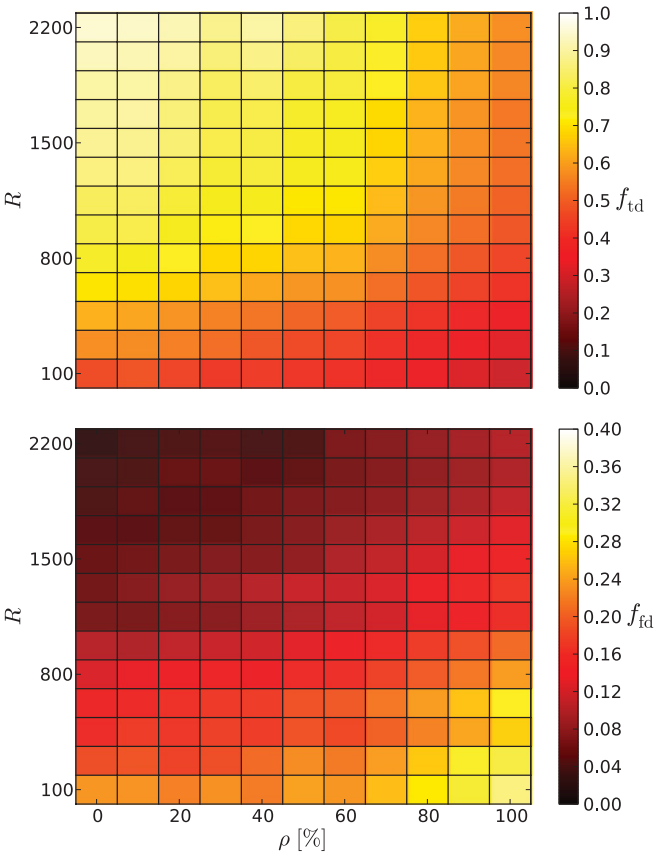

FIG. 2. (Color online) Relative number of true (f_{td}, top) and false detections (f_{fd}, bottom) of the coupling direction (cf. Fig. 1) depending on the number of realizations R and on the noise-to-signal ratio with $\rho_X = \rho_Y$. For each R and ρ we show mean values of f_{td} and f_{fd} obtained from 50 different sets of noise-contaminated Lorenz systems.

B. Event-related brain potentials

In this section we present our findings obtained from applying our method to infer directional interactions in so-called event-related brain potentials (ERPs). The electroencephalogram (EEG) reflects electrical neural activity owing to intrinsic dynamics and/or responses to external stimuli. To examine the pathways and time courses of information processing in the brain under specific conditions, numerous experiments have been developed controlling sensory or other stimuli [59,60]. The neural activity induced by this kind of stimulation leads to potential changes in the EEG. These ERPs often exhibit a sequence of multiphasic peak amplitudes after stimulus onset and extending over a time period of several 100 ms. ERPs reflect different stages of information

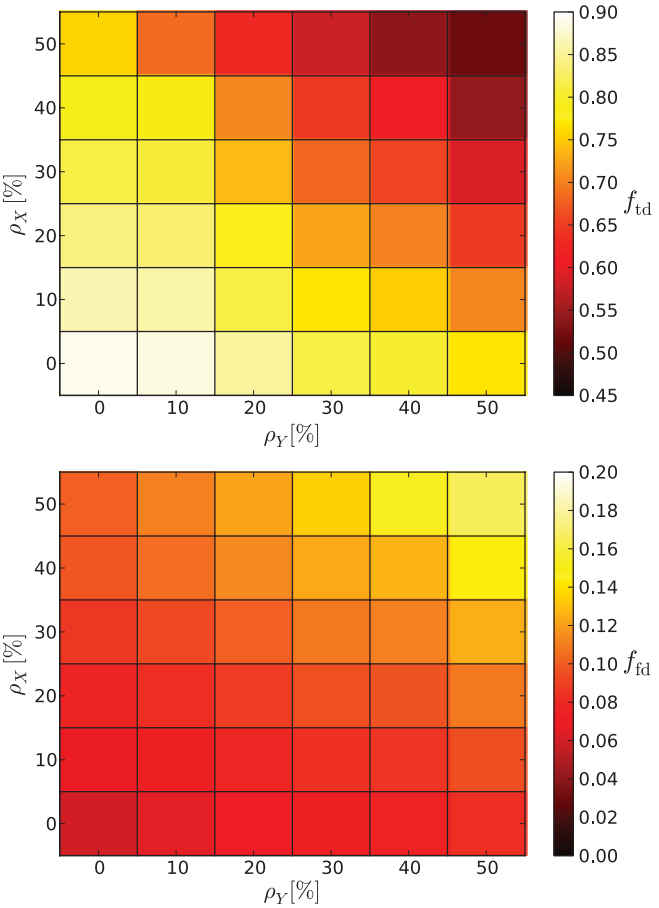

FIG. 3. (Color online) Relative number of true (f_{td}, top) and false detections (f_{fd}, bottom) of the coupling direction (cf. Fig. 1) depending on the noise-to-signal ratio for asymmetric noise contaminations. For each $\rho_{X,Y}$ we show mean values of f_{td} and f_{fd} obtained from 50 different sets of noise-contaminated Lorenz systems with $R = 2000$ realizations.

processing in the brain, and insights into the underlying neural processes can be achieved already from the analysis of specific aspects of ERPs, such as peak amplitude or moment of occurrence (latency). Because individual ERPs possess very low peak amplitudes, as compared to the ongoing EEG, multiple realizations with respect to a given stimulus are commonly averaged, assuming phase-locked responses not correlated with the ongoing EEG. In Refs. [50,61–66] data-analysis techniques have been proposed that make use of only a few measurements instead of large preprocessed ensembles.

We analyzed directional interactions in ERP data that we recorded from 12 healthy volunteers during the so-called Simon task [67]. All volunteers had signed informed consent that their data might be used and published for research purposes, and the study protocol had been approved previously by the local ethics committee. The Simon task is often used in cognitive psychology to study the effects of cognitive control and requires pressing a key with the right (left) index finger upon presentation of a red (blue) circle on a screen (diameter of circle: 1.5 cm; stimulus duration: 50 ms; presentation randomized in time and position). ERPs were acquired from $N_c = 21$ scalp electrodes arranged according to the International 10-20 system [60]. Data were sampled against a common average reference at a sampling rate of 1000 Hz by using a 16-bit analog-to-digital converter and were bandpass filtered between 0.5 and 300 Hz at 12 dB per octave. We recorded $R = 100$ trials for each of the four subtasks [red (blue) circle–left (right) index finger]. For this experiment, we mainly expect directed interactions from the occipital lobe (processing of visual information) to the frontal lobe (decision making) and from the frontal lobe to the motor area (key press) [68]. For our analyses, we concentrated on the time interval ranging from 200 ms before stimulus onset to 1000 ms after stimulus onset. The time interval ranging from 0 to 1000 ms after stimulus onset is sufficient to capture the main components of the averaged ERPs that have been described in previous studies [68–70]. With $w = 4$ [56] and $\tau = 3$ sample points [71] we estimated the time-resolved directionality index $\Delta T(n)$ for the data from all nonredundant combinations of recording sites, and eventually corrected all values with respect to the mean directionality indices estimated for the data from the prestimulus interval, which is usually taken to be a period of inactivity.

Figure 4 shows, as an example, the temporal evolution of directional interactions between the occipital lobe and the frontal lobe and between the frontal lobe and the motor area (central-parietal region). We do not differentiate between subtasks here and show values of $\Delta T(n)$ averaged over all subtasks. For this subject, we observe a preferred direction of information flow from the occipital lobe to the frontal lobe that is most pronounced during the time interval ranging from 150 to 250 ms after stimulus onset. This time frame coincides quite well with latencies of ERP components known to reflect stimulus processing within primary sensory or secondary association regions as well with stimulus evaluation processes, such as identification and classification [68]. Directional interactions between the frontal lobe and the motor area peak during the time interval ranging from 400 to 500 ms,

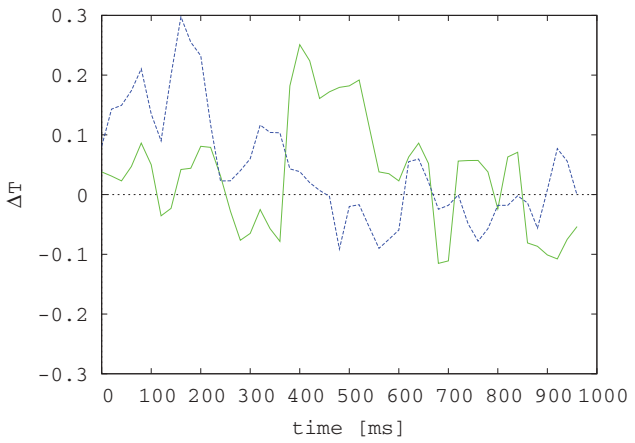

FIG. 4. (Color online) Exemplary temporal evolution of the preferred direction of information flow $\Delta T(n)$ between the occipital lobe and the frontal lobe (blue dashed line) and between the frontal lobe and the motor area (green solid line). Moving average over 20 data points (no overlap), corresponding to 20 ms. Positive values reflect directional influences of the occipital (frontal) lobe on the frontal lobe (motor area), and vice versa.

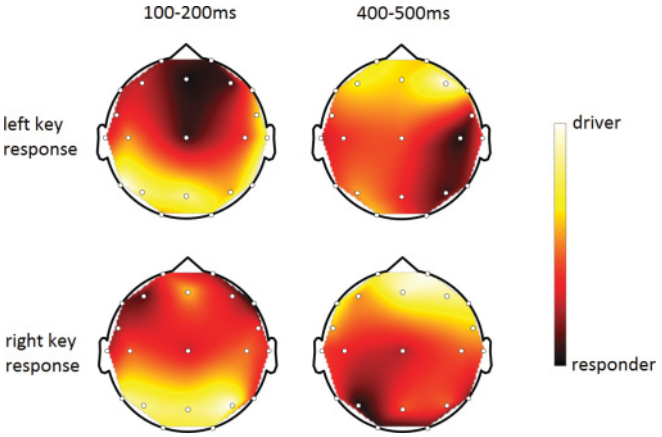

FIG. 5. (Color online) Spatial distributions of the preferred direction of information flow from each recording site to the remaining sites projected onto the surface of the head. Grand average over 12 healthy volunteers for subtasks that either required a left key (upper row) or a right key response (lower row). Left-hand column: 100–200 ms after stimulus onset; right-hand column: 400–500 ms after stimulus onset. White circles mark electrode locations.

with the frontal lobe identified as driving brain region. This time frame coincides quite well with latencies of components of the averaged ERPs known to reflect motoric processes, and the mean reaction time of this subject amounted to 421 ± 38 ms.

In Fig. 5 we show, as a grand average over all volunteers, spatial distributions of the preferred direction of information flow from each recording site c to the remaining $N_c - 1$ sites. We calculated $\Delta T(n,c) = (N_c - 1)^{-1} \sum_{c' \neq c} [\Delta T_{c \to c'}(n) - \Delta T_{c' \to c}(n)]$ for each time point n and averaged the data from the time intervals $n \in [100,200]$ ms and $n \in [400,500]$ ms. Eventually, we averaged the data for those subtasks that either involved pressing a key with the right or the left index finger, irrespective of the color of the stimulus. For the time interval 100–200 ms after stimulus onset, we observe, as expected, a preferred direction of information flow mainly from the occipital lobe to the frontal lobe, and the spatial distributions do not differ substantially between different subtasks. In contrast, for the time interval 400–500 ms after stimulus onset, we observe the frontal lobe to drive either the right motor area for subtasks that involve pressing the left index finger or the left motor area for subtasks that involve pressing the right index finger. The mean reaction time of all volunteers amounted to 442 ± 43 ms for the former and to 433 ± 47 ms for the latter subtask.

IV. CONCLUSION

We have proposed an approach that allows the time-resolved investigation of directional relationships between coupled dynamical systems from short and transient noisy time series. We have extended the concept of symbolic transfer entropy [41] for an ensemble of such time series representing multiple realizations of some interaction process and derived an index that quantifies the direction of a transient interaction. Using a surrogate-based testing scheme [43,47,72] we assessed the significance of our index. With numerical examples, which are representative of interacting chaotic systems contaminated with observational noise, we have exemplified the applicability of our approach.

Our findings obtained from an analysis of directional relationships between event-related potentials recorded non-invasively from 12 healthy volunteers underline the versatility of our approach as a tool to improve understanding of gross neural interactions underlying cognitive processes. We expect that our approach will also find applications in other scientific fields where transient couplings are considered an interesting aspect of interacting dynamical systems.

ACKNOWLEDGMENTS

We are grateful to Christiane Toepser for help with ERP data acquisition and for critical comments on earlier versions of the manuscript. This work was supported by the Deutsche Forschungsgemeinschaft (Grant No. LE660/5-1).

[1] A. S. Pikovsky, M. G. Rosenblum, and J. Kurths, *Synchronization: A Universal Concept in Nonlinear Sciences* (Cambridge University Press, Cambridge, UK, 2001).
[2] S. Boccaletti, J. Kurths, G. Osipov, D. L. Valladares, and C. S. Zhou, Phys. Rep. **366**, 1 (2002).
[3] E. Pereda, R. Quian Quiroga, and J. Bhattacharya, Prog. Neurobiol. **77**, 1 (2005).
[4] M. Winterhalder, B. Schelter, and J. Timmer, Int. J. Bifurcation Chaos Appl. Sci. Eng. **17**, 3725 (2007).
[5] G. Nolte, A. Ziehe, V. V. Nikulin, A. Schlögl, N. Krämer, T. Brismar, and K.-R. Müller, Phys. Rev. Lett. **100**, 234101 (2008).
[6] F. Gans, A. Y. Schumann, J. W. Kantelhardt, T. Penzel, and I. Fietze, Phys. Rev. Lett. **102**, 098701 (2009).
[7] M. G. Rosenblum, A. S. Pikovsky, J. Kurths, C. Schaefer, and P. A. Tass, in *Handbook of Biological Physics*, edited by F. Moss and S. Gielen (Elsevier Science, Amsterdam, 2001), pp. 297–321.
[8] D. A. Smirnov and B. P. Bezruchko, Phys. Rev. E **68**, 046209 (2003).
[9] L. Cimponeriu, M. Rosenblum, and A. Pikovsky, Phys. Rev. E **70**, 046213 (2004).
[10] D. A. Smirnov and R. G. Andrzejak, Phys. Rev. E **71**, 036207 (2005).
[11] D. A. Smirnov, M. B. Bodrov, J. L. P. Velazquez, R. A. Wennberg, and B. P. Bezruchko, Chaos **15**, 024102 (2005).
[12] B. Schelter, M. Winterhalder, T. Maiwald, A. Brandt, A. Schad, A. Schulze-Bonhage, and J. Timmer, Chaos **16**, 013108 (2006).
[13] B. Kralemann, L. Cimponeriu, M. Rosenblum, A. S. Pikovsky, and R. Mrowka, Phys. Rev. E **76**, 055201 (2007).
[14] D. Smirnov, B. Schelter, M. Winterhalder, and J. Timmer, Chaos **17**, 013111 (2007).
[15] H. Osterhage, F. Mormann, M. Staniek, and K. Lehnertz, Int. J. Bifurcation Chaos Appl. Sci. Eng. **17**, 3539 (2007).

[16] H. Osterhage, F. Mormann, T. Wagner, and K. Lehnertz, Phys. Rev. E **77**, 011914 (2008).
[17] J. Nawrath, M. C. Romano, M. Thiel, I. Z. Kiss, M. Wickramasinghe, J. Timmer, J. Kurths, and B. Schelter, Phys. Rev. Lett. **104**, 038701 (2010).
[18] S. J. Schiff, P. So, T. Chang, R. E. Burke, and T. Sauer, Phys. Rev. E **54**, 6708 (1996).
[19] J. Arnhold, P. Grassberger, K. Lehnertz, and C. E. Elger, Physica D **134**, 419 (1999).
[20] R. Quian Quiroga, J. Arnhold, and P. Grassberger, Phys. Rev. E **61**, 5142 (2000).
[21] D. Krug, H. Osterhage, C. E. Elger, and K. Lehnertz, Phys. Rev. E **76**, 041916 (2007).
[22] M. C. Romano, M. Thiel, J. Kurths, and C. Grebogi, Phys. Rev. E **76**, 036211 (2007).
[23] L. Faes, A. Porta, and G. Nollo, Phys. Rev. E **78**, 026201 (2008).
[24] D. Chicharro and R. G. Andrzejak, Phys. Rev. E **80**, 026217 (2009).
[25] Y. Hirata and K. Aihara, Phys. Rev. E **81**, 016203 (2010).
[26] C. Granger, Econometrica **37**, 424 (1969).
[27] M. Dhamala, G. Rangarajan, and M. Ding, Phys. Rev. Lett. **100**, 018701 (2008).
[28] D. Marinazzo, M. Pellicoro, and S. Stramaglia, Phys. Rev. Lett. **100**, 144103 (2008).
[29] J. Prusseit and K. Lehnertz, Phys. Rev. E **77**, 041914 (2008).
[30] A. Bahraminasab, F. Ghasemi, A. Stefanovska, P. V. E. McClintock, and R. Friedrich, New J. Phys. **11**, 103051 (2009).
[31] K. Hlaváčková-Schindler, M. Paluš, M. Vejmelka, and J. Bhattacharya, Phys. Rep. **441**, 1 (2007).
[32] M. Paluš and M. Vejmelka, Phys. Rev. E **75**, 056211 (2007).
[33] M. Vejmelka and M. Paluš, Phys. Rev. E **77**, 026214 (2008).
[34] J. Jamšek, M. Paluš, and A. Stefanovska, Phys. Rev. E **81**, 036207 (2010).
[35] T. Schreiber, Phys. Rev. Lett. **85**, 461 (2000).
[36] A. Kaiser and T. Schreiber, Physica D **166**, 43 (2002).
[37] R. Marschinski and H. Kantz, Eur. Phys. J. B **30**, 275 (2002).
[38] J. M. Nichols, M. Seaver, S. T. Trickey, M. D. Todd, C. Olson, and L. Overbey, Phys. Rev. E **72**, 046217 (2005).
[39] P. F. Verdes, Phys. Rev. E **72**, 026222 (2005).
[40] M. Lungarella, A. Pitti, and Y. Kuniyoshi, Phys. Rev. E **76**, 056117 (2007).
[41] M. Staniek and K. Lehnertz, Phys. Rev. Lett. **100**, 158101 (2008).
[42] M. A. Kramer, E. Edwards, M. Soltani, M. S. Berger, R. T. Knight, and A. J. Szeri, Phys. Rev. E **70**, 011914 (2004).
[43] R. G. Andrzejak, A. Ledberg, and G. Deco, New J. Phys. **8**, 6 (2006).
[44] S. Łeski and D. K. Wójcik, Phys. Rev. E **78**, 041918 (2008).
[45] C. Komalapriya, M. Thiel, M. C. Romano, N. Marwan, U. Schwarz, and J. Kurths, Phys. Rev. E **78**, 066217 (2008).
[46] K. Ishiguro, N. Otsu, M. Lungarella, and Y. Kuniyoshi, Phys. Rev. E **77**, 026216 (2008).
[47] T. Wagner, J. Fell, and K. Lehnertz, New J. Phys. **12**, 053031 (2010).
[48] I. M. Jánosi and T. Tél, Phys. Rev. E **49**, 2756 (1994).
[49] M. Dhamala, Y.-C. Lai, and E. J. Kostelich, Phys. Rev. E **64**, 056207 (2001).
[50] A. Effern, K. Lehnertz, T. Schreiber, T. Grunwald, P. David, and C. E. Elger, Physica D **140**, 257 (2000).
[51] S. Stausberg and K. Lehnertz, Phys. Rev. E **79**, 041914 (2009).
[52] L. Barnett, A. B. Barrett, and A. K. Seth, Phys. Rev. Lett. **103**, 238701 (2009).
[53] C. Bandt and B. Pompe, Phys. Rev. Lett. **88**, 174102 (2002).
[54] T. Kreuz, F. Mormann, R. G. Andrzejak, A. Kraskov, K. Lehnertz, and P. Grassberger, Physica D **225**, 29 (2007).
[55] W. H. Press, S. A. Teukolsky, W. T. Vetterling, and B. P. Flannery, *Numerical Recipes in C*, 2nd ed. (Cambridge University Press, Cambridge, UK, 2002).
[56] M. Staniek and K. Lehnertz, Int. J. Bifurcation Chaos Appl. Sci. Eng. **17**, 3729 (2007).
[57] Z. Albo, G. V. Di Prisco, Y. Chen, G. Rangarajan, W. Truccolo, J. Feng, R. P. Vertes, and M. Ding, Biol. Cybern. **90**, 318 (2004).
[58] G. Nolte, O. Bai, L. Wheaton, Z. Mari, S. Vorbach, and M. Hallett, Clin. Neurophysiol. **115**, 2292 (2004).
[59] *Event-Related Brain Potentials*, edited by E. Callaway, P. Tueting, and S. Koslow (Academic, New York, 1978).
[60] *Electroencephalography: Basic Principles, Clinical Applications, and Related Fields*, edited by E. Niedermeyer and F. Lopes da Silva (Lippincott Williams and Williams, Philadelphia, 2005).
[61] P. Graben, J. D. Saddy, M. Schlesewsky, and J. Kurths, Phys. Rev. E **62**, 5518 (2000).
[62] A. Effern, K. Lehnertz, G. Fernandez, T. Grunwald, P. David, and C. E. Elger, Clin. Neurophysiol. **111**, 2255 (2000).
[63] R. Quian Quiroga and H. Garcia, Clin. Neurophysiol. **114**, 376 (2003).
[64] N. Marwan and A. Meinke, Int. J. Bifurcation Chaos **14**, 761 (2004).
[65] S. Schinkel, N. Marwan, and J. Kurths, Cogn. Neurodyn. **1**, 317 (2007).
[66] S. Schinkel, N. Marwan, and J. Kurths, J. Physiol. (Paris) **103**, 315 (2009).
[67] J. R. Simon, J. Exp. Psychol. **81**, 174 (1969).
[68] R. D. Melara, H. Wang, K.-P. L. Vu, and R. W. Proctor, Brain Res. **1215**, 147 (2008).
[69] F. Valle–Inclán, Biol. Psychol. **43**, 147 (1996).
[70] D. Galashan, M. Wittfoth, T. Fehr, and M. Herrmann, Biol. Psychol. **78**, 246 (2008).
[71] D. Kugiumtzis, Physica D **95**, 13 (1996).
[72] J. Theiler, Phys. Lett. A **196**, 335 (1995).